Spatial scale and site fidelity shape the correlation between blood and feather mercury in a riverine bird

Authors

Lara Hinninger[a,b,*], Molly Ohse[a,c], Blandine Doligez[d,‡], Pierre Bize[a,c,‡]

[a]*Swiss Ornithological Institute, Seerose 1, 6204 Sempach, Switzerland*

[b]*University of Zurich, Winterthurerstrasse 190, 8057 Zurich, Switzerland*

[c]*Department of Ecology and Evolution, University of Lausanne, Biophore, 1015 Lausanne, Switzerland*

[d]*Université Lyon 1, CNRS, LBBE, UMR 5558, Villeurbanne, France*

* Corresponding author. E-mail address: lara.hinninger@vogelwarte.ch

‡ Shared senior authorship

Contact + ORCIDs

L.H.: Lara Hinninger (lara.hinninger@vogelwarte.ch): 0009-0003-7490-4280

M.O.: Molly Ohse (molly.ohse@vogelwarte.ch): 0009-0006-2303-4723

P.B.: Pierre Bize (pierre.bize@vogelwarte.ch): 0000-0002-6759-4371

B.D.: Blandine Doligez (blandine.doligez@univ-lyon1.fr): 0000-0003-3015-5022

Abstract

Blood and feathers are the non-lethal matrices most used to monitor mercury (Hg) in birds. Blood reflects recent intake at the sampling site, whereas feathers record exposure during moult, possibly elsewhere. Their correspondence should therefore vary with spatial scale and with site-fidelity. We tested this using 229 paired red blood cell and feather samples from 199 adult white-throated dippers (*Cinclus cinclus*) of mixed sex and age on eight rivers in the Chartreuse Mountains, France. Bivariate Bayesian mixed models estimated blood–feather correlations in Hg concentrations at the population level, among and within rivers, and by site fidelity. River explained about half the variance in both matrices, whereas territory explained more variance in blood than in feather Hg (intra-class correlation 0.24 vs. 0.03). Blood and feather Hg were moderately correlated (r_{pop} = 0.45 [95% highest density interval 0.31, 0.59]), combining strong correspondence among rivers (r_{river} = 0.88 [0.60, 1.00]) with weak correspondence within rivers ($r_{within\text{-}river}$ = 0.09 [−0.07, 0.27]). Correspondence was stronger in site-faithful than in other birds (r_{pop} = 0.67 vs. 0.19). Within rivers, breeding partners were strongly correlated in blood but not in feather Hg ($r_{within\text{-}river}$ = 0.70 vs. 0.14). Concentrations in blood Hg, but not feather Hg, declined by 56% within four months. Feathers suit comparisons among rivers or regions, particularly in site-faithful adults, whereas blood is better suited to territories and to birds of unknown moult location, provided that sampling date is standardised or modelled. Blood–feather correlations should be reported at the spatial scale of inference.

Keywords

Mercury, sampling matrices, bioindicator validation, spatial scale, avian toxicology, white-throated dipper

1. Introduction

Mercury (Hg) is a persistent environmental contaminant whose distribution has been profoundly altered by human activities (Panagos et al., 2021; Pompeani et al., 2018). Even environmentally relevant concentrations can disrupt oxidative balance, impair behaviour and reduce reproductive success (Ackerman et al., 2024; Chételat et al., 2020), and higher exposure can cause complete reproductive failure (Ackerman et al., 2016; Bjedov et al., 2025; Depew et al., 2012), reducing fitness and threatening population persistence (Chételat et al., 2020). Risks are greatest for animals feeding on aquatic resources, because microbial processes in aquatic systems convert inorganic Hg into methylmercury (MeHg), which biomagnifies through food webs (Chételat et al., 2020; Mahat et al., 2025). Monitoring Hg in biota is therefore a global priority and is required under the United Nations Minamata Convention on Mercury (UNEP, 2013).

Birds are valuable bioindicators: many species occupy high trophic positions and show fitness costs of contamination (Albert et al., 2019; Bjedov et al., 2025; Rutkowska et al., 2018). Their Hg contamination can be measured in several matrices that integrate exposure over different time windows (Ackerman et al., 2024; Chételat et al., 2020; Eagles-Smith et al., 2008). Internal tissues have well-defined toxicity benchmarks (Chételat et al., 2020) but require destructive sampling, so avian biomonitoring increasingly relies on blood and feathers (Low et al., 2020; Zabala et al., 2019). Blood reflects dietary intake over the preceding days to weeks and thus Hg bioavailability at the bird's most recent location (Furness et al., 1986). Its strong correlations with Hg in eggs and internal tissues make it the indicator of choice for health and reproductive risk (Ackerman et al., 2024).

Feathers, in contrast, incorporate Hg during growth and are metabolically inert thereafter (Bottini et al., 2021; Furness et al., 1986), recording exposure during moult, including Hg remobilised from internal stores (Honda et al., 1986; Renedo et al., 2021). Simpler sampling, sample preparation, and storage make them attractive for biomonitoring (Peterson et al., 2019). Interpreting feather Hg, however, requires species-specific knowledge (Chételat et al., 2020; Low et al., 2020), because it depends on when and where the feather was grown (Bertram et al., 2022, 2026), on feather type (Bertram et al., 2026; Peterson et al., 2019) and on how Hg is transferred from blood into growing feathers (Bottini et al., 2021). Consequently, correlations between feather and blood Hg in adult birds have often been reported as weak or inconsistent (Ackerman et al., 2019; Low et al., 2020). Strong correlations do occur under some conditions. In captive song sparrows (*Melospiza melodia*), Hg in growing feathers closely tracked blood Hg ($r \approx 0.98$; Bottini et al., 2021). In field studies, however, feathers are usually sampled months after moult, whereas blood reflects recent exposure (Furness et al., 1986), so strong correlations are expected mainly in species that have small home ranges and experience limited change in exposure (Ackerman et al., 2012; Chételat et al., 2020), as reported for California clapper rails ($r \approx 0.87$; *Rallus obsoletus;* Ackerman et al., 2012) and Carolina wrens ($r \approx 0.94$; *Thryothorus ludovicianus;* Jackson et al., 2011). However, in a closely related

resident species, the marsh wren (*Cistothorus palustris*), Hartman et al. (2013) found correlations of r ≈ 0.10–0.63 across feather types and sexes in adult birds.

Beyond the blood to feather transfer during growth, blood–feather correspondence depends on the circumstances of sampling, which we refer to collectively as the ecological context. Two aspects are central. The first is the spatial scale of comparison: local area means of blood and feather Hg can track the same geographic pattern even when individual values within a site correspond only weakly (Edmonds et al., 2010; Zabala et al., 2019). The second is whether a feather was grown at the same place as, and close in time to, the blood sample, which depends on whether a bird remained at its moult site until it was sampled, that is, on its site fidelity, a trait that can differ among individuals even within resident species (Bertram et al., 2026; Low et al., 2020; Peterson et al., 2019). Because environmental Hg exposure varies both spatially and seasonally (Hartman et al., 2017; Zabala et al., 2019), feathers grown elsewhere or months before sampling need not reflect current exposure. Partly for this reason, fully grown feathers were excluded when avian toxicity reference values were derived, as their Hg often reflects a temporal mismatch with the endpoint measured (Ackerman et al., 2024), and their exposure window must be considered before they are used to infer exposure at particular locations or times (e.g. Chételat et al., 2020; Low et al., 2020).

To our knowledge, no field study has examined both factors together, partitioning blood–feather correlations across spatial scales while accounting for where the sampled feather was grown. It therefore remains unclear whether the weak correlations often reported in adult birds reflect an inherent limitation of feathers as indicators or, at least in part, a mismatch between the scale and context of sampling. The white-throated dipper (*Cinclus cinclus*) is well suited to test how the ecological context shapes blood–feather correspondence, that is, the strength of their correlation. Most dippers hold small, linear river territories year-round and are exposed to Hg through their aquatic diet (Silverthorn et al., 2018; Tyler & Ormerod, 1994). Individuals differ in site fidelity (Galarza et al., 2023), and the river network provides a natural hierarchy of spatial scales. Breeding partners share a territory, which allows a test of whether a shared location produces similar exposure. In our study population in the Chartreuse Mountains, France, long-term monitoring of territory use, sex and age allows us to estimate where most birds grew the sampled feather, and so whether feather and blood reflect the same location.

Using paired blood and feather samples from adult dippers of mixed sex and age (yearlings to ≥ 5 years), we asked under which conditions blood and feather Hg correspond. Because individual traits, seasonal timing and spatial structure can all influence Hg accumulation (Chételat et al., 2020), we first (i) quantified their contributions to variation in each matrix. We then (ii) estimated blood–feather correlations at the population level, among rivers and within rivers, predicting weaker correspondence within rivers. We tested whether correspondence was stronger (iii) in birds that remained site-faithful between moult and capture and (iv) for feathers grown in the moult after, rather than before, blood sampling. Finally, (v) we estimated correlations between breeding partners within each matrix, predicting greater similarity between partners in blood than in feather Hg if shared location drives exposure. Identifying these conditions indicates at which

spatial scales and for which individuals the more easily collected feathers can complement blood in monitoring.

2. Methods

2.1 Study species and study area

White-throated dippers are small passerines (50–70 g; this study) living near fast-flowing rivers across Eurasia (Tyler & Ormerod, 1994). They feed mainly on benthic macroinvertebrates, such as caddisfly, mayfly and stonefly larvae, and on small fish, and are widely used as indicators of river water quality (Silverthorn et al., 2018; Tyler & Ormerod, 1994). Adults defend linear territories of 300–2500 m along rivers and remain highly faithful to them across seasons and years (Crowther et al., 2018; Tyler & Ormerod, 1994). Young birds often leave their natal territory between June and October (Tyler & Ormerod, 1994), and usually settle within a few kilometres of their natal site (Galarza et al., 2023). Moult differs between age classes (Jenni et al., 2020): adults undergo a complete post-breeding moult starting mid-June (B.D., personal observation), whereas juveniles undergo a partial post-juvenile moult (Jenni et al., 2020). Undertail coverts, the feathers sampled here, are replaced in both age classes.

The study population in the Chartreuse Mountains, France (Fig. 1), has been monitored since 2014 by ringing adults and nestlings. The river network (200–1100 m a.s.l.) spans a gradient from formerly industrialised, now largely urbanised valleys to remote catchments. Capture locations were assigned to eight river units (hereafter rivers; 15–46 samples each; Fig. 1). The region has among the highest topsoil Hg concentrations in Europe, with legacy industrial sources contributing to small-scale variation in Hg bioavailability (Panagos et al., 2021).

2.2 Field methods

From mid-January to mid-May in 2024 and 2025, adult dippers were caught with mist nets at active territories. Birds were weighed and ringed with a metal ring provided by the French national ringing scheme (C.R.B.P.O., Muséum National d'Histoire Naturelle, Paris) and a unique colour-ring combination. Adults were sexed from body size and the presence of a brood patch (Tyler & Ormerod, 1994), and aged as yearlings (born in the previous calendar year) or older adults from plumage (Jenni et al., 2020). Exact ages were determined from ringing records. At each bird's first capture in a year, we collected 200–250 µl of blood from the metatarsal vein and plucked two undertail covert feathers for Hg analyses (sampling and storage details in Appendix A.1).

Breeding pairs were identified from colour-ring combinations read on videos recorded during nest building and nestling feeding. From approximately 200 pairs monitored annually, about 55 per year were included in this study, selected to span ages and rivers. The final dataset comprised 229 paired blood and feather samples from 199 individuals (99 females, 100 males) on 109 territories in eight rivers. It is a mixed-sex,

mixed-age sample covering different adult ages. Because 30 birds were sampled in both years, group sizes are given as n samples (N individuals).

2.3 Mercury analysis

We measured total Hg in red blood cells, which carry over 90% of Hg in avian blood (Bond & Robertson, 2015), and in undertail coverts. Because MeHg accounts for most of the Hg in avian blood and feathers (84–99%; Mahat et al., 2025; Renedo et al., 2018), total Hg can be used as a proxy for this most biologically active form (Chételat et al., 2020). We therefore refer to total Hg in our red blood cell and feather samples as blood Hg and feather Hg, and use 'Hg' alone for mercury in general.

For the laboratory analysis, about 15 µl of thawed red blood cells were dried on filter paper, and feathers were washed and oven-dried. Total Hg was quantified in dried blood strips and whole feathers with a Direct Mercury Analyser (DMA-80 evo, Milestone Srl, Sorisole, Italy) by thermal decomposition, gold amalgamation and atomic absorption spectrometry (U.S. EPA, 2007), and is reported in $mg \cdot kg^{-1}$ dry weight (dw). Duplicate analyses gave a coefficient of variation of 2.3 ± 2.6% (mean ± standard deviation (SD); n = 36) for blood and 14.6 ± 15.9% (n = 39) for feathers. Feather duplicates were two different feathers from the same bird, so their variation includes among-feather differences as well as analytical error. Sample preparation, instrument settings and quality control are given in Appendix A.1.

2.4 Statistical analysis

Analyses were run in R (version 4.6.1; R Core Team, 2026). Blood and feather Hg were natural log-transformed, and age and Julian capture date were standardised (mean = 0, SD = 1 across all 229 samples). All models were Bayesian Gaussian mixed models fitted with brms (Bürkner, 2017). Table A.2 lists the response, fixed and random effects and sample size of every main model. Models used the default weakly informative priors of *brms* (Bürkner, 2021) and four chains of 12,000 iterations (6,000 warm-up), thinned by a factor of 2, giving 12,000 posterior draws. We report posterior means with 95% highest density intervals (HDI) computed with *bayestestR* (Makowski, Ben-Shachar, & Lüdecke, 2019) and the probability of direction (Pd), the proportion of the posterior with the same sign as its median (Makowski, Ben-Shachar, & Lüdecke, 2019). Pd relates to a two-sided p-value as $p \approx 2 \times (1 - Pd)$ (Makowski, Ben-Shachar, Chen, et al., 2019). We treated $Pd \geq 0.975$ as evidence and $0.95 \leq Pd < 0.975$ as weak evidence for an effect. Model fit was summarised with conditional and marginal Bayesian R^2 (Gelman et al., 2019). Convergence and sampler behaviour were checked with R-hat, bulk and tail effective sample sizes, divergent transitions, and trace and posterior predictive plots from *bayesplot* (Gabry et al., 2019). For comparisons between correlations from different models, we computed the difference between the two correlations in each posterior draw, following Gerritsma et al. (2023).

2.4.1 Sources of variation in blood and feather Hg

First, we assessed sources of variation in Hg measured in each matrix. For both blood and feathers, we fitted a univariate model including age (1 to ≥ 5 years), sex, year and capture date as fixed effects, and random intercepts for capture territory (109 levels) nested in river (8 levels) and for bird identity (199 levels). We compared this linear model with three extended models that added quadratic terms of age and date (quadratic model), their interactions with sex (interaction model), or both (full model; Table A.2).

We compared the four candidate models by their expected log predictive density (ELPD), estimated with Pareto-smoothed importance-sampling leave-one-out cross-validation (PSIS-LOO) in the loo package (Vehtari et al., 2017). PSIS-LOO was unreliable (Pareto k > 0.7) for 22–31 of the 229 observations in the blood models and for 3–6 in the feather models, depending on the candidate model. Most of these were birds sampled once or birds on territories sampled only once, whose individual or territory random effects each rest on a single observation. We therefore refitted each model once per problematic observation and replaced the approximate ELPD contributions of these observations with exact ones. An extended model was preferred over the linear model only if its ELPD was higher by more than 4 units and by more than twice the standard error of the difference (Sivula et al., 2025).

Intra-class correlation coefficients (ICC), the proportion of variance at each random-effect level, were estimated for the selected model with the *performance* package (Lüdecke et al., 2021). Because 22 of the 30 birds sampled in both years were captured on the same territory, territory and individual variance were partly confounded (Ohse et al., 2026). We therefore refitted both models with one randomly chosen sample per bird (n = N = 199; Table A.3).

2.4.2 Blood–feather Hg correlations across scales and sampling contexts

To quantify how closely blood and feather Hg correspond when sampled from one bird, we fitted bivariate mixed models in which blood Hg and feather Hg were the two responses. Each response had its own fixed effects: those with at least weak evidence in the univariate models (Pd ≥ 0.95), plus year for both responses to account for interannual variation. Bird identity was fitted as a random intercept for each response. Because most birds were sampled only once, among- and within-individual covariance could not be separated (Dingemanse & Dochtermann, 2013).

The quantity of interest is the residual correlation between the two responses, i.e. the correlation that remains after the fixed and random effects have been accounted for. We separated spatial scales by fitting two versions of the model that differed only in their random effects (Table A.2). In the population model, bird identity was the only random effect, giving the population-level correlation (r_{pop}: do birds with higher blood Hg also have higher feather Hg across the study area?). The river-structured model added correlated river intercepts for the two responses, which split the covariance into an among-river correlation (r_{river}: do rivers where mean blood Hg is high also have higher mean feather Hg?) and a within-river correlation ($r_{within\text{-}river}$: within the same river, does a bird with higher blood Hg than expected also have higher feather Hg than

expected?). We did not fit a random intercept for territory, because most territories held only one or two samples. Consequently, r_{pop} combines covariance among rivers, territories and individuals, whereas $r_{within\text{-}river}$ combines covariance among territories and individuals within rivers . Because r_{river} is estimated from only eight rivers and is bounded at 1, we interpret it from its lower HDI limit. Finally, to estimate river-specific correlations, we reused the fitted river-structured model: for every posterior draw, we split the observation-level residuals by river and computed the blood–feather correlation within each river (Table A.4).

Next, we assessed whether site fidelity affects blood–feather correspondence by fitting the above models separately to site-faithful and not site-faithful birds. Where feathers were grown was not observed directly, so we used each bird's last known location before the preceding moult as its presumed feather growth location (hereafter, moult location) and compared it with the capture location. The last known location was the breeding territory in the preceding year (older adults, n = 110 samples), the last capture in that year if no breeding attempt was recorded (n = 18), or the natal territory (n = 63; for one further yearling, its capture site as a juvenile). Birds captured within 1 km of this location, measured along the river network (OpenStreetMap Wiki contributors, 2026), were classified as site-faithful (n = 118, N = 103). All others, together with the 37 birds first ringed as yearlings, which had most likely hatched outside the exhaustively monitored population, were classified as not site-faithful (n = 111, N = 108). For yearlings, the natal territory only approximates the moult location, because the post-juvenile moult coincides with natal dispersal. Any misclassification would mix the two groups and thus reduce, rather than inflate, the difference between them. Because only three not site-faithful birds were sampled in both years, bird identity was omitted from the models of not site-faithful birds (Table A.2). The 1 km threshold approximates the mean territory length reported by Tyler and Ormerod (1994). To test whether our conclusions depended on the choice of this threshold, we refitted the models with alternative thresholds of 0.5, 2 and 5 km (Table A.5). Furthermore, because site fidelity and age class are strongly associated in dippers, we refitted the same models separately for older adults and yearlings (Table A.6).

Finally, we tested whether the timing of feather growth relative to blood sampling affects the correspondence. Using the 30 birds sampled in both years, we correlated blood Hg in 2024 with (1) the feather collected at the same capture, grown in the 2023 moult, before the blood sample, and (2) the feather collected at the 2025 recapture, grown in the 2024 moult, after the blood sample but in the same year. We expected feather (2) to correspond more closely to blood, as it reflects exposure in the same year. Given the small sample, we estimated only the population-level correlation (Table A.2).

2.4.3 Correlations between breeding pair members within each matrix

To test the role of shared location, we correlated Hg between the members of 110 breeding pairs (96 females and 96 males; some birds bred in both years). For each matrix, we fitted a bivariate model with female and male Hg of the same pair as the two responses and estimated the correlation at the same three spatial scales as in Section 2.4.2, assigning rivers by nest location. Fixed effects were selected as in Section 2.4.2 (Pd ≥ 0.95 in the univariate models), with year included for both responses (Table A.2). Random

intercepts for female and male identity accounted for birds sampled in both years. The pair identity was not modelled because only five pairs were sampled twice. To identify pairs in which both pair members had grown their feathers at the same location, we recorded whether their moult locations (Section 2.4.2) lay within 1 km of each other. Again, birds first ringed as yearlings were assumed to have moulted outside the study area and thus at a different location from their partner. To assess whether the correlation strengths differ based on the choice of the threshold, we refitted the models with alternative thresholds of 1, 2, 5 km for bird that moulted within the same river (Table A.7).

3. Results

We analysed 229 simultaneously collected blood and feather samples from 199 individual dippers across the two study years. Mean ± SD blood Hg was 0.48 ± 0.25 $mg \cdot kg^{-1}$ dw (range 0.12–1.59) and feather Hg was 1.82 ± 1.04 $mg \cdot kg^{-1}$ dw (range 0.40–7.23).

3.1 Sources of variation in blood and feather Hg

For both matrices, no extended model had clearly higher predictive accuracy than the linear model, and the full blood model had clearly lower predictive accuracy (ΔELPD = −4.4 ± 1.7; Appendix A.2), so the linear models were retained. Blood Hg did not differ detectably between the sexes, whereas there was weak evidence that feather Hg was lower in males than in females (Pd = 0.96, Table 1). Neither blood nor feather Hg showed a detectable trend with age (Table 1).

Blood Hg showed pronounced temporal variation, decreasing linearly on a log scale over the four-month sampling season: blood Hg fell by 56% [42, 66]. Blood was also a further 12% [4, 19] lower in 2025 than in 2024 (Table 1). Feather Hg, by contrast, varied neither within the sampling season nor between years (Table 1).

Spatial structure captured by the random effects accounted for the largest share of variation in both matrices, reflected in conditional Bayesian R^2 values far exceeding the marginal values (Table 1). Variation in blood Hg was structured by both river (ICC = 0.55) and territory (ICC = 0.24), whereas feather Hg was structured mainly by river (ICC = 0.50), with little additional territory-level variation (ICC = 0.03). Bird identity accounted for little variance in either matrix (ICC ≤ 0.05; Table 1). Including each bird only once gave a similar variance structure (Table A.3).

Table 1. Sources of variation in blood and feather Hg (aim i). *Univariate Bayesian mixed-effects models were fitted separately to log-transformed blood and feather Hg (mg·kg^{-1} dw; n = 229 samples from N = 199 birds). Upper block: fixed-effect posterior means with 95% highest density intervals (HDI) and probability of direction (Pd); age and capture date were standardised (mean 0, SD 1). Lower block: random-effect standard deviations (SD) with their 95% HDI, intra-class correlation coefficients (ICC) and Bayesian R^2. Values in bold indicate Pd ≥ 0.975.*

	log blood Hg (mg·kg^{-1} dw)			**log feather Hg (mg·kg^{-1} dw)**		
Fixed effects	Estimate	95% HDI	Pd	Estimate	95% HDI	Pd
Intercept	**−0.85**	**[−1.18, −0.52]**	**1.00**	**0.49**	**[0.13, 0.83]**	**0.99**
age	0.03	[−0.02, 0.07]	0.89	0.01	[−0.05, 0.08]	0.66
sex [male]	−0.05	[−0.13, 0.02]	0.91	−0.10	[−0.22, 0.01]	0.96
year [2025]	**−0.13**	**[−0.21, −0.05]**	**1.00**	−0.09	[−0.21, 0.03]	0.93
date	**−0.17**	[**−0.23, −0.11]**	**1.00**	0.02	[−0.05, 0.09]	0.73
Random effects	SD	95% HDI	ICC	SD	95% HDI	ICC
river (N = 8)	0.42	[0.19, 0.72]	0.55	0.45	[0.20, 0.76]	0.50
territory (N = 109)	0.28	[0.22, 0.34]	0.24	0.11	[0.00, 0.22]	0.03
bird identity (N = 199)	0.08	[0.00, 0.17]	0.02	0.14	[0.00, 0.28]	0.05
Residual	0.25	[0.20, 0.29]		0.40	[0.33, 0.47]	
$R^2_{conditional}$ / $R^2_{marginal}$	0.80 / 0.14			0.48 / 0.03		

3.2 Blood–feather Hg correlations across scales and sampling contexts

The blood–feather correlation depended on spatial scale (Table 2; Fig. 2). It was moderate at the population level (r_{pop} = 0.45 [0.31, 0.59]) and weak within rivers ($r_{within\text{-}river}$ = 0.09 [−0.07, 0.27]), whereas among rivers it was strong (r_{river} = 0.88 [0.60, 1.00]). When evaluating the correlation per river, we found that correlations ranged from −0.17 to 0.24 and were positive only in Morge (Table A.4).

Correspondence depended strongly on site fidelity. Among site-faithful individuals, blood and feather Hg were strongly correlated at the population level and remained positively correlated within rivers (r_{pop} = 0.67, r_{river} = 0.91 [0.68, 1.00], $r_{within\text{-}river}$ = 0.35; Table 2; Fig. 3A). Among birds that were not site-faithful, the population-level correlation was weak (r_{pop} = 0.19), the among-river correlation was moderate but imprecise (r_{river} = 0.58 [−0.04, 1.00]; Table 2; Fig. 3A), and there was no evidence of a within-river correlation (Table 2; Fig. 3A). Posterior comparisons showed clearly stronger correlations in site-faithful than in not site-faithful birds at the population level (Δ = 0.48 [0.25, 0.71]) and within rivers (Δ = 0.36 [0.06, 0.65]), but not among rivers (Table 2). Repeating the analyses by age class, a grouping which is closely associated with site fidelity in this population, gave similar but slightly smaller differences (Table A.6). The contrast was also robust to the distance threshold used to define site fidelity: with thresholds of 0.5, 2 and 5 km, correlations remained higher in site-faithful than in not site-faithful birds at the population level (Δr_{pop} = 0.47 to 0.58, Pd = 1.00 in all three cases) and, less clearly, within rivers ($\Delta r_{within\text{-}river}$ = 0.28 to 0.43, Pd = 0.97 to 0.99), whereas no differences among rivers were detected (Table A.5).

The timing of feather growth relative to blood sampling had no strong effect on the correlation. In the 30 dippers sampled in both years, blood Hg showed only weak evidence of a correlation with Hg in the feather grown before the blood sample, in the 2023 moult (r_{pop} = 0.35 [0.01, 0.66], Table 2; Fig. 3B), and was positively correlated with Hg in the feather grown after the blood sample, in the 2024 moult (r_{pop} = 0.46 [0.16, 0.74]; Table 2; Fig. 3B). The difference ran in the predicted direction, with stronger correlation for feathers grown in the moult after, rather than before, blood sampling, yet the posterior comparison did not support it (Δ = −0.12 [−0.54, 0.35]; Table 2).

Table 2. Blood–feather and within-pair correlations in Hg (aims ii–v). *Correlations (r) are posterior means [95% highest density interval, HDI] with probability of direction (Pd) from bivariate Bayesian mixed-effects models, estimated at the population level (r_{pop}), among rivers (r_{river}) and within rivers ($r_{within\text{-}river}$). Upper block: blood–feather Hg correlations for all birds (aim ii), by site fidelity (aim iii) and by the timing of feather growth relative to blood sampling (aim iv). Lower block: correlations between the male and female member of a breeding pair within each matrix (aim v). Δ is the difference between the two rows above it (site-faithful − not site-faithful; grown before − grown after; blood − feather), computed in each posterior draw. Values in bold indicate Pd ≥ 0.975. n = number of samples; N = number of individuals; f = female; m = male.*

Correlations (r)			Population level (r_{pop})		Among rivers (r_{river})		Within-river ($r_{within\text{-}river}$)	
Aim		n (N)	mean [95% HDI]	Pd	mean [95% HDI]	Pd	mean [95% HDI]	Pd
Blood–feather Hg correlations								
(ii)	*all birds*	229 (199)	**0.45 [0.31, 0.59]**	**1.00**	**0.88 [0.60, 1.00]**	**1.00**	0.09 [−0.07, 0.27]	0.87
(iii)	*site fidelity*							
	site-faithful	118 (103)	**0.67 [0.54, 0.81]**	**1.00**	**0.91 [0.68, 1.00]**	**1.00**	**0.35 [0.12, 0.56]**	**1.00**
	not site-faithful	111 (108)	**0.19 [0.01, 0.37]**	**0.98**	0.58 [−0.04, 1.00]	0.94	−0.01 [−0.20, 0.18]	0.55
	difference Δ		**0.48 [0.25, 0.71]**	**1.00**	0.33 [−0.19, 1.09]	0.90	**0.36 [0.06, 0.65]**	**0.99**
(iv)	*feather growth timing relative to blood*							
	grown before (2023 moult)	30 (30)	0.35 [0.01, 0.66]	0.97				
	grown after (2024 moult)	30 (30)	**0.46 [0.16, 0.74]**	**1.00**				
	difference Δ		−0.12 [−0.54, 0.35]	0.70				
Between breeding pair members								
(v)	*same breeding location*							
	blood	110 (f, m = 96)	**0.79 [0.67, 0.94]**	**1.00**	**0.84 [0.48, 1.00]**	**0.99**	**0.70 [0.52, 0.87]**	**1.00**
	feather	110 (f, m = 96)	**0.50 [0.25, 0.76]**	**1.00**	**0.77 [0.29, 1.00]**	**0.99**	0.14 [−0.12, 0.40]	0.85
	difference Δ		**0.29 [0.01, 0.58]**	**0.98**	0.07 [−0.49, 0.76]	0.60	**0.57 [0.25, 0.89]**	**1.00**

3.3 Correlations between breeding pair members within each matrix

Correlations between the two breeding pair members differed between the matrices and with spatial scale (Table 2; Fig. 4). At the population level, pair member correlations were strong for blood (r_{pop} = 0.79) and moderate for feathers (r_{pop} = 0.50). Among rivers, they were clearly positive in both matrices (r_{river} = 0.84 [0.48, 1.00] for blood and 0.77 [0.29, 1.00] for feathers). Within rivers, blood Hg remained strongly correlated between pair members ($r_{within\text{-}river}$ = 0.70), whereas feather Hg did not ($r_{within\text{-}river}$ = 0.14). Partner similarity was therefore higher in blood than in feather Hg at the population level (Δ = 0.29 [0.01, 0.58]) and, most markedly, within rivers (Δ = 0.57 [0.25, 0.89]), but not among rivers. Restricting the analysis to pairs whose moult locations lay within 0.5 to 5 km of each other, or in the same river, did not increase the similarity of partners' feather Hg (r_{pop} = 0.34 to 0.42; $r_{within\text{-}river}$ = −0.07 to 0.10; Table A.7).

4. Discussion

Blood and feather Hg corresponded closely in white-throated dippers under two ecological conditions: when birds were compared across rivers rather than within one, and when feathers had grown where the blood was sampled. Spatial structure, and river in particular, accounted for most of the variation in both matrices, with an additional territory-level component mainly in blood. Accordingly, the two matrices identified the same rivers as having higher Hg, but not the same birds within a river. Within-river correspondence was low overall but increased when comparisons were restricted to site-faithful birds. Blood Hg was also strongly correlated between breeding pair members sharing a territory, even within rivers. Taken together, these results indicate that where a bird lives and feeds, rather than its age or sex, accounts for most of the variation in its Hg exposure in this system, and that blood resolves this spatial variation at a finer resolution than feathers.

4.1 Spatial structure, not age or sex, accounts for most Hg variation

Spatial structure accounted for most of the variation in Hg in both matrices, whereas age and sex contributed comparatively little (Table 1). Blood Hg varied strongly among rivers and also among territories within rivers, despite the close proximity of neighbouring territories, whereas feather Hg was structured mainly at the river level. Blood Hg therefore reflected both broad- and fine-scale spatial heterogeneity in exposure, whereas feather Hg in our sample reflected mainly the broader, river-specific pattern. This is consistent with the spatial structuring reported in other avian biomonitoring studies (Hartman et al., 2013; Zabala et al., 2019) and with capture location predicting blood but not feather Hg in Forster's terns (*Sterna forsteri*, Ackerman et al., 2008).

The weak territory signal in feathers probably reflects the composition of our sample. In adult females aged two years or more from the same population, which had mostly moulted on their established territory, feather Hg did vary among territories, although less than among individuals and rivers (Ohse et al., 2026). Our mixed-sex, mixed-age sample from the same population, in contrast, included 101 samples from yearlings, most of which were classed as not site-faithful (Section 2.4.2). Because these feathers probably record exposure elsewhere, they reduce any territory signal.

In addition to the strong spatial signal, blood Hg declined substantially across the sampling period, falling by more than half over four months. A similar decline of about 60% from spring to autumn was reported in grebes, in which sampling date predicted blood Hg more strongly than moult (Hartman et al., 2017). Feather Hg showed no seasonal variation, consistent with feathers recording exposure during a discrete moulting period independent of capture date (Bottini et al., 2021; Chételat et al., 2020). The absence of a date trend in feathers also makes it unlikely that the blood decline is an artefact of sampling less contaminated rivers later in the season. The most obvious explanations for blood Hg declines, depuration through moult and through maternal transfer to eggs (Bottini et al., 2021; Chételat et al., 2020), are unlikely here: all individuals were sampled before moult, and most females before egg laying. A more likely explanation is seasonal

change in Hg intake or physiological processes such as redistribution of Hg from blood to internal tissues as body condition changes (Chételat et al., 2020; Eagles-Smith et al., 2008; Zabala et al., 2019). Resampling dippers early and late within a single season, combined with measurements of Hg bioavailability on the same territories, would help separate a within-individual decline from differences between the individuals sampled, and changes in intake from physiological redistribution (Anderson et al., 2009; Chételat et al., 2020). For monitoring, this decline means that blood Hg can be compared among individuals, territories or rivers only if sampling dates are standardised or modelled.

Neither blood nor feather Hg showed a detectable trend with age, and only feather Hg showed weak evidence of a sex difference, being slightly lower in males than in females. This contrasts with the age- and sex-related patterns often reported in birds, in which Hg burdens increase with age and are lower in females that offload Hg during egg laying (Beccardi et al., 2025; Bertram et al., 2024; Chételat et al., 2020). In this population, age and sex therefore added little to the spatial signal. For monitoring, this means that samples need to be stratified by location, but pooling males and females is unlikely to bias the comparison of exposure much.

4.2 Blood–feather correlations depend on spatial scale

The moderate population-level blood–feather correlation in dippers (r_{pop} = 0.45; Table 2) falls within the range reported for other resident or territorial species: weaker than in Carolina wrens (r ≈ 0.94; Jackson et al., 2011) and common loons (*Gavia immer*, r ≈ 0.59; Scheuhammer et al., 1998), but stronger than the lowest estimates for marsh wrens (r ≈ 0.10; Hartman et al., 2013). These comparisons are approximate, for two reasons. First, the estimates were obtained with different approaches: other studies typically report simple correlations or regressions of (log-transformed) concentrations, whereas r_{pop} is the residual correlation after accounting for the fixed effects and bird identity (Section 2.4.2). Second, a blood–feather correlation is not a fixed property of a species. It expresses the size of the shared exposure signal relative to all other sources of variation, and therefore depends also on the exposure range sampled (Goodwin and Leech, 2006). That range usually widens with the spatial scale of sampling, although not necessarily: contamination may be uniform across a whole catchment, or vary steeply over a few hundred metres around a point source.

In our population, river was the largest single source of variance in both matrices (ICC = 0.55 and 0.50; Table 1), although about half of the variance still lay within rivers. As predicted, the two matrices corresponded among rivers but only weakly within them: river means of blood and feather Hg were strongly correlated (r_{river} = 0.88, lower HDI limit 0.60), whereas within a river a bird's blood and feather Hg corresponded only weakly ($r_{within\text{-}river}$ = 0.09; Fig. 2; Table 2). Averaging over the 15–46 samples of a river cancels most of the variation specific to one matrix, such as among-feather variation in feather Hg or short-term dietary variation in blood Hg, and leaves the exposure signal that both matrices share; in a single bird, this shared signal is weakened by matrix-specific variation. The same pattern was reported in great egret

nestlings (Zabala et al., 2019), in which colony means of Hg correlated closely among albumen, blood and feathers (R^2 > 0.53), whereas concentrations from the same individual did not (R^2 < 0.23). For biomonitoring, a population-level blood–feather correlation therefore has to be interpreted at the spatial scale at which it was obtained: in our system, it supports feather Hg for comparisons among rivers and regions, whereas inference about the current exposure of individual birds within a river requires blood or knowledge of where the feather grew.

4.3 Site fidelity shapes blood–feather correspondence

As predicted, site fidelity, and hence a shared location for feather growth and blood sampling, was associated with stronger blood–feather correspondence. Correlations were substantially higher in site-faithful than in not site-faithful birds, both at the population level (r_{pop} = 0.67 vs. 0.19; Fig. 3A; Table 2) and within rivers ($r_{within\text{-}river}$ = 0.35 vs. −0.01; Table 2). This classification assumes that each bird moulted at its last known location; birds that moved before or during moult would have been misclassified, which would weaken rather than inflate the contrast, so the true difference may be larger. The clearly positive within-river correlation in site-faithful birds indicates that the two matrices remain correlated even at this fine spatial scale when both reflect the same location, so the weak overall within-river estimate is not an intrinsic limit of feather Hg. In birds that were not site-faithful, capture and moult locations probably differed, so the two samples integrated exposure at two places and the correspondence was weak. Nevertheless, even without a shared location, correlations may arise. For example, through consistent individual foraging, as in migratory common terns, in which body feathers grown in the wintering area correlated with breeding-season blood Hg (Bertram et al., 2026).

In dippers, site fidelity is closely linked to age. Young birds commonly leave their natal area after fledging (Galarza et al., 2024; Tyler & Ormerod, 1994), so the undertail coverts of yearlings had often grown far from where the birds were later captured. Older adults, by contrast, typically remain on the same territory across years (110 of 128 samples from older adults in this study were site-faithful) and replace all their feathers in a complete post-breeding moult, thus feathers and blood reflect exposure at the territory they defend. Site fidelity and age class were accordingly strongly overlapping in our population. Repeating the models by age class instead of site fidelity yielded similar but slightly smaller differences (Table A.6). In practice, this makes age a useful field proxy: age in dippers is far easier to determine than site fidelity, and it can identify the individuals, or the subsets of a population, in which feather Hg is most likely to reflect exposure at the sampling location. Such a proxy is species-specific, however. In marsh wrens, blood–feather correlations tended to be stronger in juveniles and adult females than in adult males (Hartman et al., 2013). Age is therefore informative only in combination with species-specific knowledge on for example dispersal, moult strategy and dietary preferences (Ackerman et al., 2008; Chételat et al., 2020).

Feathers grown after blood sampling corresponded more closely to blood Hg than feathers from the previous moult (0.46 vs 0.35), but the difference was uncertain, so our data neither confirm nor rule out an

effect of growth timing. One explanation for why both feathers tracked blood Hg is that 22 of the 30 recaptured birds stayed on the same territory in both years. Where territories differ consistently in exposure between years (Ohse et al., 2026), a feather from either moult reflects the same exposure, and growth timing should matter little. This is consistent with the stronger blood–feather correspondence in site-faithful birds. Growth timing should matter more in birds that move between moults, which were too few in our recapture sample to test.

4.4 Breeding pair members are highly similar in blood Hg

Breeding partners resembled each other strongly in blood Hg, and this similarity remained high within rivers (r_{pop} = 0.79, $r_{within\text{-}river}$ = 0.70; Table 2). Because blood Hg reflects dietary intake over the preceding days to weeks (Bottini et al., 2021; Chételat et al., 2020), and dipper pair members forage on the same territory, a shared feeding area is the most parsimonious explanation for their similarity. In common terns, by contrast, partner similarity in blood Hg was much weaker ($r \approx 0.25$) and was attributed to courtship feeding (Bertram et al., 2025). The similarity in dippers does not simply reflect partners being sampled at the same point in the seasonal decline of blood Hg, because each partner's Hg was adjusted for its own capture date and for year, nor age-assortative mating, because Hg showed no detectable relationship with age (Table 1). Partners could also resemble each other if individuals of similar quality, for example as a result of favourable early-life conditions, paired with each other and settled on preferred territories (Bruinzeel et al., 2006). Such pairing, however, should then also make partners similar in feather Hg, which was less strongly the case in our sample (Table 2). Partner similarity in blood Hg is therefore consistent with current Hg exposure being set largely at the territory scale.

As predicted, partners resembled each other less in feather than in blood Hg, most markedly within rivers ($r_{within\text{-}river}$ = 0.14 vs. 0.70; Table 2). Feathers record where each bird moulted, and only 39 of the 110 pairs had moulted within 1 km of each other. To test whether this explains the lower similarity of feathers, we restricted the analysis to pairs that had moulted within 0.5 to 5 km of each other, or in the same river. This did not raise the within-river correlation of their feather Hg ($r_{within\text{-}river}$ = −0.07 to 0.10; Table A.7), so differing moult locations alone do not explain the weak similarity of feathers within rivers. These subsets were small (36 to 67 pairs), and estimates showed large HDIs. Such correlation analyses would be interesting to repeat in a larger sample. Among rivers, the feather correlation remained positive and did not differ clearly from blood (r_{river} = 0.77 vs. 0.84; lower HDI limits 0.29 and 0.48; Table 2), consistent with both partners having moulted in the same river in 67 of the 110 pairs, which maintains the river-level signal. Within a river, the feather Hg of one partner is therefore only weakly informative about that of the other, beyond what is already known based on the river. In contrast, blood Hg differed among territories within the same river, which supports its use for monitoring at the territory scale.

5. Conclusion

Whether feather Hg corresponded to blood Hg depended on the ecological context: on the spatial scale of comparison and on whether the feather had grown where the blood was sampled. In white-throated dippers, blood and feather Hg identified the same rivers as more contaminated, but not the same birds within a river. Within rivers, correspondence was clearly stronger in site-faithful birds, whose feathers had grown near the place of blood sampling. Breeding partners, which share a territory, were strongly similar in blood Hg but not in feather Hg within rivers.

These results lead to four recommendations for using blood and feathers as Hg indicators. First, feathers are well suited to comparing rivers or regions, preferably in birds that moulted where they were sampled. In species in which site fidelity increases with age, as in dippers, age class can serve as a field proxy to identify site-faithful birds. Second, blood is better suited to assessing recent exposure on a territory, particularly in birds of unknown moult location. Third, as blood Hg declined by more than half over four months in our study population, blood-based monitoring should standardise sampling dates or account for their effects statistically, as done in the present study. Where possible, analyses should also consider physiological state, including breeding stage and body condition. Fourth, blood–feather correlations should be reported at the spatial scale of inference, because a single population-level correlation combines strong correspondence among rivers with weak correspondence within them.

Without Hg data from prey or the abiotic environment, we cannot determine how closely either matrix tracks environmental contamination. The correlation estimates themselves depend on the range of exposure sampled and should not be generalised to other systems, even for the same species. What remains valid is the pattern: site fidelity, moult and spatial scale determine when the two matrices carry the same information.

Blood and feather Hg are therefore complementary rather than interchangeable. Their correspondence in other systems should be anticipated from a species' site fidelity, moult pattern and the exposure range sampled, rather than assumed. Knowing when feathers can complement blood, and when they cannot, will improve avian Hg monitoring and its contribution to evaluating the Minamata Convention on Mercury (UNEP, 2013).

Ethics statement

This work was conducted under permits from the C.R.B.P.O. (Personal Ringing Programme n° 655), DREAL (Isère and Savoie; authorisations 38-2018-0601015, 2018-727, 38-2023-0807-00007, 74-2023-09-22-00007), and approved by the Université Lyon 1 ethical committee (APAFIS28729202012171619277 8 v4).

CRediT authorship contribution statement

L.H.: Conceptualization, Methodology, Validation, Formal analysis, Investigation, Data Curation, Writing - Original Draft, Writing - Review & Editing, Visualization, Funding acquisition (supporting).
M.O.: Conceptualization, Methodology (supporting), Validation, Formal analysis (supporting), Investigation, Data Curation (supporting), Writing - Review & Editing, Supervision, Project administration (supporting).
P.B.: Conceptualization, Methodology (supporting), Validation, Formal analysis (supporting), Investigation, Resources, Writing - Review & Editing, Supervision, Project administration (supporting), Funding acquisition.
B.D.: Conceptualization, Methodology (supporting), Validation, Formal analysis (supporting), Resources, Data Curation, Writing - Review & Editing, Supervision, Project administration, Funding acquisition.

Funding information

This research was funded by the Swiss National Science Foundation (grant no. 212971 to P.B.), the Centre National de la Recherche Scientifique (CNRS; Interdisciplinary Office MITI, AAP “Long term monitoring” 2024 to B.D.), the Chartreuse Fund, via the Association du Réseau Rivières Sauvages and the Chartreuse Regional Nature Park (2023–2024 to B.D.), and the Association for the Study of Animal Behaviour (ASAB, 2024 to B.D.). This work is part of the “Sites Rivières Sauvages” (“Wild rivers site”) label awarded to the Guiers Mort, one of the study rivers, since 2019. L.H. was additionally supported by a scholarship from Science Alumni UZH. The funders had no role in study design, data collection and analysis, decision to publish, or preparation of the manuscript.

Open data and code

The data and R code supporting this study will be archived in the Vogelwarte.ch Open Repository and Archive on Zenodo and assigned a DOI upon acceptance.

For peer review, the data and code are available in an anonymised repository:
https://anonymous.4open.science/r/Dipper_BF_data_code-B6FA

Declaration of generative AI and AI-assisted technologies in the manuscript preparation process

During the preparation of this work, the authors used Scite.ai (Research Solutions Company) in order to identify relevant papers for the literature review and discussion. The authors also used Claude (Anthropic, Sonnet and Opus) in order to improve the language and readability of the text, to assist with debugging R code, and to prepare the shared data and code repository. After using these tools, the authors reviewed and edited the content as needed and take full responsibility for the content of the published article.

Acknowledgements

We thank all the students, volunteers, and field assistants who contributed to the extensive long-term monitoring of white-throated dippers through the annual fieldwork coordinated by B. D., and in particular A. Cillard and M. Bastianelli for their participation in adult catching and sampling in 2024–2025. We are grateful for having access to the mercury analyser in the cLab at the Institute of Geography, University of Bern. We especially thank Eva Anthamatten for her invaluable support and assistance with the mercury measurements.

References

Ackerman, J. T., Eagles-Smith, C. A., Herzog, M. P., Hartman, C. A., Peterson, S. H., Evers, D. C., Jackson, A. K., Elliott, J. E., Vander Pol, S. S., & Bryan, C. E. (2016). Avian mercury exposure and toxicological risk across western North America: A synthesis. *Science of The Total Environment*, *568*, 749–769. https://doi.org/10.1016/j.scitotenv.2016.03.071

Ackerman, J. T., Eagles-Smith, C. A., Takekawa, J. Y., Bluso, J. D., & Adelsbach, T. L. (2008). Mercury concentrations in blood and feathers of prebreeding Forster's terns in relation to space use of San Francisco Bay, California, USA, habitats. *Environmental Toxicology and Chemistry*, *27*(4), 897–908. https://doi.org/10.1897/07-230.1

Ackerman, J. T., Hartman, C. A., & Herzog, M. P. (2019). Mercury contamination in resident and migrant songbirds and potential effects on body condition. *Environmental Pollution*, *246*, 797–810. https://doi.org/10.1016/j.envpol.2018.11.060

Ackerman, J. T., Overton, C. T., Casazza, M. L., Takekawa, J. Y., Eagles-Smith, C. A., Keister, R. A., & Herzog, M. P. (2012). Does mercury contamination reduce body condition of endangered California clapper rails? *Environmental Pollution*, *162*, 439–448. https://doi.org/10.1016/j.envpol.2011.12.004

Ackerman, J. T., Peterson, S. H., Herzog, M. P., & Yee, J. L. (2024). Methylmercury effects on birds: A review, meta-analysis, and development of toxicity reference values for injury assessment based on tissue residues and diet. *Environmental Toxicology and Chemistry*, *43*(6), 1195–1241. https://doi.org/10.1002/etc.5858

Albert, C., Renedo, M., Bustamante, P., & Fort, J. (2019). Using blood and feathers to investigate large-scale Hg contamination in Arctic seabirds: A review. *Environmental Research*, *177*, 108588. https://doi.org/10.1016/j.envres.2019.108588

Anderson, O., Phillips, R., McDonald, R., Shore, R., McGill, R., & Bearhop, S. (2009). Influence of trophic position and foraging range on mercury levels within a seabird community. *Marine Ecology Progress Series*, *375*, 277–288. https://doi.org/10.3354/meps07784

Beccardi, M., Bertram, J., Bouwhuis, S., Salmón, P., Schupp, P. J., & Vedder, O. (2025). Experimental evidence for maternal offloading of mercury pollution via reproduction. *Environmental Pollution*, *385*, 127121. https://doi.org/10.1016/j.envpol.2025.127121

Bertram, J., Bichet, C., Moiron, M., Kürten, Nathalie, Schupp, P. J., & Bouwhuis, S. (2025). Parental blood mercury levels are correlated, and predictive of those in eggs in a long-lived seabird. *Environmental Research*, *275*, 121437. https://doi.org/10.1016/j.envres.2025.121437

Bertram, J., Bichet, C., Moiron, M., Schupp, P. J., & Bouwhuis, S. (2024). Sex- and age-specific mercury accumulation in a long-lived seabird. *Science of The Total Environment*, *927*, 172330. https://doi.org/10.1016/j.scitotenv.2024.172330

Bertram, J., Garsi, E., Bichet, C., Kürten, N., Schupp, P. J., & Bouwhuis, S. (2026). Differential mercury accumulation and links to blood mercury levels across feather types in a long-lived seabird. *Environmental Monitoring and Assessment*, *198*(5), 460. https://doi.org/10.1007/s10661-026-15310-4

Bertram, J., Kürten, N., Bichet, C., Schupp, P. J., & Bouwhuis, S. (2022). Mercury contamination level is repeatable and predicted by wintering area in a long-distance migratory seabird. *Environmental Pollution*, *313*, 120107. https://doi.org/10.1016/j.envpol.2022.120107

Bjedov, D., Sudarić Bogojević, M., Bernal-Alviz, J., Klobučar, G., Bourdineaud, J.-P., Aarif, K. M., & Mikuška, A. (2025). An integrative approach to assessing the impact of mercury (Hg) on avian behaviour: From molecule to movement. *Journal of Xenobiotics*, *15*(4), 117. https://doi.org/10.3390/jox15040117

Bond, A. L., & Robertson, G. J. (2015). Mercury concentrations in multiple tissues of Arctic Iceland Gulls (*Larus glaucoides*) wintering in Newfoundland. *Arctic Science*, *1*(1). https://doi.org/10.1139/as-2015-0004

Bottini, C. L. J., MacDougall-Shackleton, S. A., Branfireun, B. A., & Hobson, K. A. (2021). Feathers accurately reflect blood mercury at time of feather growth in a songbird. *Science of The Total Environment*, *775*, 145739. https://doi.org/10.1016/j.scitotenv.2021.145739

586 Bruinzeel, L. W., van de Pol, M., & Trierweiler, C. (2006). Competitive abilities of oystercatchers
587 (*Haematopus ostralegus*) occupying territories of different quality. *Journal of Ornithology*, *147*(3),
588 457–463. https://doi.org/10.1007/s10336-005-0037-1
589 Bürkner, P.-C. (2017). brms: An R package for Bayesian multilevel models using Stan. *Journal of*
590 *Statistical Software*, *80*(1), 1–28. https://doi.org/10.18637/jss.v080.i01
591 Bürkner, P.-C. (2021). Bayesian item response modeling in R with brms and Stan. *Journal of Statistical*
592 *Software*, *100*(5), 1–54. https://doi.org/10.18637/jss.v100.i05
593 Chételat, J., Ackerman, J. T., Eagles-Smith, C. A., & Hebert, C. E. (2020). Methylmercury exposure in
594 wildlife: A review of the ecological and physiological processes affecting contaminant
595 concentrations and their interpretation. *Science of The Total Environment*, *711*, 135117.
596 https://doi.org/10.1016/j.scitotenv.2019.135117
597 Crowther, W., Magoolagan, L., Mawby, P. J., Whitehead, F. A., Wright, P. M., & Sharp, S. P. (2018).
598 Winter territoriality and its implications for the breeding ecology of white-throated dippers *Cinclus*
599 *cinclus*. *Bird Study*, *65*(4), 471–477. https://doi.org/10.1080/00063657.2018.1541963
600 Depew, D. C., Basu, N., Burgess, N. M., Campbell, L. M., Evers, D. C., Grasman, K. A., & Scheuhammer,
601 A. M. (2012). Derivation of screening benchmarks for dietary methylmercury exposure for the
602 common loon (*Gavia immer*): Rationale for use in ecological risk assessment. *Environmental*
603 *Toxicology and Chemistry*, *31*(10), 2399–2407. https://doi.org/10.1002/etc.1971
604 Dingemanse, N. J., & Dochtermann, N. A. (2013). Quantifying individual variation in behaviour: Mixed-
605 effect modelling approaches. *Journal of Animal Ecology*, *82*(1), 39–54.
606 https://doi.org/10.1111/1365-2656.12013
607 Eagles-Smith, C. A., Ackerman, J. T., Adelsbach, T. L., Takekawa, J. Y., Miles, A. K., & Keister, R. A.
608 (2008). Mercury correlations among six tissues for four waterbird species breeding in San
609 Francisco Bay, California, USA. *Environmental Toxicology and Chemistry*, *27*(10), 2136–2153.
610 https://doi.org/10.1897/08-038.1
611 Edmonds, S. T., Evers, D. C., Cristol, D. A., Mettke-Hofmann, C., Powell, L. L., McGann, A. J., Armiger, J.
612 W., Lane, O. P., Tessler, D. F., Newell, P., Heyden, K., & O'Driscoll, N. J. (2010). Geographic and

seasonal variation in mercury exposure of the declining rusty blackbird. *The Condor*, *112*(4), 789–799. https://doi.org/10.1525/cond.2010.100145

Furness, R. W., Muirhead, S. J., & Woodburn, M. (1986). Using bird feathers to measure mercury in the environment: Relationships between mercury content and moult. *Marine Pollution Bulletin*, *17*(1), 27–30. https://doi.org/10.1016/0025-326X(86)90801-5

Gabry, J., Simpson, D., Vehtari, A., Betancourt, M., & Gelman, A. (2019). Visualization in Bayesian workflow. *Journal of the Royal Statistical Society Series A: Statistics in Society*, *182*(2), 389–402. https://doi.org/10.1111/rssa.12378

Galarza, A., Betanzos-Lejarraga, L., & Arizaga, J. (2024). Apparent survival and dispersal in a White-throated Dipper (*Cinclus cinclus*) population from northern Iberia. *Ornis Fennica*, 00–00. https://doi.org/10.51812/of.142115

Galarza, A., Betanzos-Lejarraga, L., & Rodriguez, P. (2023). Natal and breeding dispersal of the White-throated Dipper *Cinclus cinclus* in coastal rivers of the northern Iberian Peninsula. *Ringing & Migration*, *38*(1–2), 38–43. https://doi.org/10.1080/03078698.2023.2287559

Gelman, A., Goodrich, B., Gabry, J., & Vehtari, A. (2019). R-squared for Bayesian Regression Models. *The American Statistician*, *73*(3), 307–309. https://doi.org/10.1080/00031305.2018.1549100

Gerritsma, Y. H., Driessen, M. M. G., & Verhulst, S. (2023). Zebra finch behaviour differs consistently between individuals but is not affected by early life adversity. *Animal Behaviour*, *199*, 79–94. https://doi.org/10.1016/j.anbehav.2023.02.014

Goodwin, L. D., & Leech, N. L. (2006). Understanding Correlation: Factors That Affect the Size of r. *The Journal of Experimental Education*, *74*(3), 249–266. https://doi.org/10.3200/JEXE.74.3.249-266

Hartman, C. A., Ackerman, J. T., Herring, G., Isanhart, J., & Herzog, M. (2013). Marsh wrens as bioindicators of mercury in wetlands of Great Salt Lake: Do blood and feathers reflect site-specific exposure risk to bird reproduction? *Environmental Science & Technology*, *47*(12), 6597–6605. https://doi.org/10.1021/es400910x

Hartman, C. A., Ackerman, J. T., Herzog, M. P., & Eagles-Smith, C. A. (2017). Season, molt, and body size influence mercury concentrations in grebes. *Environmental Pollution*, *229*, 29–39. https://doi.org/10.1016/j.envpol.2017.05.058

Honda, K., Nasu, T., & Tatsukawa, R. (1986). Seasonal changes in mercury accumulation in the black-eared kite, *Milvus migrans lineatus*. *Environmental Pollution Series A, Ecological and Biological*, *42*(4), 325–334. https://doi.org/10.1016/0143-1471(86)90016-4

Jackson, A. K., Evers, D. C., Etterson, M. A., Condon, A. M., Folsom, S. B., Detweiler, J., Schmerfeld, J., & Cristol, D. A. (2011). Mercury exposure affects the reproductive success of a free-living terrestrial songbird, the Carolina Wren (*Thryothorus ludovicianus*). *The Auk*, *128*(4), 759–769. https://doi.org/10.1525/auk.2011.11106

Jenni, L., Winkler, R., & Degen, T. (2020). Moult and ageing of European passerine*s* (2nd ed.). Helm.

Low, K. E., Ramsden, D. K., Jackson, A. K., Emery, C., Robinson, W. D., Randolph, J., & Eagles-Smith, C. A. (2020). Songbird feathers as indicators of mercury exposure: High variability and low predictive power suggest limitations. *Ecotoxicology*, *29*(8), 1281–1292. https://doi.org/10.1007/s10646-019-02052-y

Lüdecke, D., Ben-Shachar, M., Patil, I., Waggoner, P., & Makowski, D. (2021). performance: An R package for assessment, comparison and testing of statistical models. *Journal of Open Source Software*, *6*(60), 3139. https://doi.org/10.21105/joss.03139

Mahat, S., Almasi, B., Ingrid S. Kjelsen, Marmet, D. S., Heckel, G., Roulin, A., Buser, A. M., & Mestrot, A. (2025). Mercury accumulation and biomagnification in the barn owl (*Tyto alba*) food chain. *Journal of Hazardous Materials*, *492*, 138269. https://doi.org/10.1016/j.jhazmat.2025.138269

Makowski, D., Ben-Shachar, M., & Lüdecke, D. (2019). bayestestR: Describing effects and their uncertainty, existence and significance within the Bayesian framework. *Journal of Open Source Software*, *4*(40), 1541. https://doi.org/10.21105/joss.01541

Makowski, D., Ben-Shachar, M. S., Chen, S. H. A., & Lüdecke, D. (2019). Indices of Effect Existence and Significance in the Bayesian Framework. *Frontiers in Psychology*, *10*, 2767. https://doi.org/10.3389/fpsyg.2019.02767

Ohse, M., Hinninger, L., Norton, G., Doligez, B., & Bize, P. (2026). *Repeated measures of mercury concentrations demonstrate persistent territory-level contamination and stable individual differences in exposure in a riverine bird predator*. In Review. https://doi.org/10.21203/rs.3.rs-10804699/v1.

OpenStreetMap contributors. (2026). OpenStreetMap [Data set]. Retrieved October 10, 2026, from https://www.openstreetmap.org

Panagos, P., Jiskra, M., Borrelli, P., Liakos, L., & Ballabio, C. (2021). Mercury in European topsoils: Anthropogenic sources, stocks and fluxes. *Environmental Research*, *201*, 111556. https://doi.org/10.1016/j.envres.2021.111556

Peterson, S. H., Ackerman, J. T., Toney, M., & Herzog, M. P. (2019). Mercury concentrations vary within and among individual bird feathers: A critical evaluation and guidelines for feather use in mercury monitoring programs. *Environmental Toxicology and Chemistry*, *38*(6), 1164–1187. https://doi.org/10.1002/etc.4430

Pompeani, D. P., Cooke, C. A., Abbott, M. B., & Drevnick, P. E. (2018). Climate, fire, and vegetation mediate mercury delivery to midlatitude lakes over the Holocene. *Environmental Science & Technology*, *52*(15), 8157–8164. https://doi.org/10.1021/acs.est.8b01523

R Core Team. (2026). *R: a language and environment for statistical computing* [Manual]. R Foundation for Statistical Computing. https://doi.org/10.32614/R.manuals

Renedo, M., Amouroux, D., Duval, B., Carravieri, A., Tessier, E., Barre, J., Bérail, S., Pedrero, Z., Cherel, Y., & Bustamante, P. (2018). Seabird tissues as efficient biomonitoring tools for Hg isotopic investigations: Implications of using blood and feathers from chicks and adults. *Environmental Science & Technology*, *52*(7), 4227–4234. https://doi.org/10.1021/acs.est.8b00422

Renedo, M., Pedrero, Z., Amouroux, D., Cherel, Y., & Bustamante, P. (2021). Mercury isotopes of key tissues document mercury metabolic processes in seabirds. *Chemosphere*, *263*, 127777. https://doi.org/10.1016/j.chemosphere.2020.127777

Rutkowska, M., Plotka-Wasylka, J., Lubinska-Szczygel, M., Różańska, A., Możejko-Ciesielska, J., & Namieśnik, J. (2018). Birds' feathers—Suitable samples for determination of environmental pollutants. *TrAC Trends in Analytical Chemistry*, *109*, 97–115. https://doi.org/10.1016/j.trac.2018.09.022

Scheuhammer, A. M., Atchison, C. M., Wong, A. H. K., & Evers, D. C. (1998). Mercury exposure in breeding Common loons (*Gavia immer*) in central Ontario, Canada. *Environmental Toxicology and Chemistry*, *17*(2), 191–196. https://doi.org/10.1002/etc.5620170208

Silverthorn, V. M., Bishop, C. A., Jardine, T., Elliott, J. E., & Morrissey, C. A. (2018). Impact of flow diversion by run-of-river dams on American dipper diet and mercury exposure. *Environmental Toxicology and Chemistry*, *37*(2), 411–426. https://doi.org/10.1002/etc.3961

Sivula, T., Magnusson, M., & Vehtari, A. (2025). Uncertainty in Bayesian Leave-One-Out Cross-Validation Based Model Comparison. *Bayesian Analysis*, *1*. https://doi.org/10.1214/25-BA1569

Tyler, S., & Ormerod, S. (1994). *The Dippers*. Bloomsbury Publishing Plc.

UNEP. (2013, January 11). *Global Mercury Assessment 2013: Sources, emissions, releases, and environmental transport | UNEP - UN Environment Programme.* https://www.unep.org/resources/report/global-mercury-assessment-2013-sources-emissions-releases-and-environmental

U.S. EPA. (2007). *Method 7473: Mercury in solids and solutions by thermal decomposition, amalgamation, and atomic absorption spectrophotometry*. U.S. EPA. https://www.epa.gov/sites/default/files/2015-12/documents/7473.pdf

Vehtari, A., Gelman, A., & Gabry, J. (2017). Practical Bayesian model evaluation using leave-one-out cross-validation and WAIC. *Statistics and Computing*, *27*(5), 1413–1432. https://doi.org/10.1007/s11222-016-9696-4

Zabala, J., Rodriguez-Jorquera, I. A., Orzechowski, S. C., & Frederick, P. (2019). Non-lethal sampling of avian indicators reveals reliable geographic signals of mercury despite highly dynamic patterns of exposure in a large wetland. *Environmental Pollution*, *247*, 577–585. https://doi.org/10.1016/j.envpol.2019.01.057

Figures and Legends

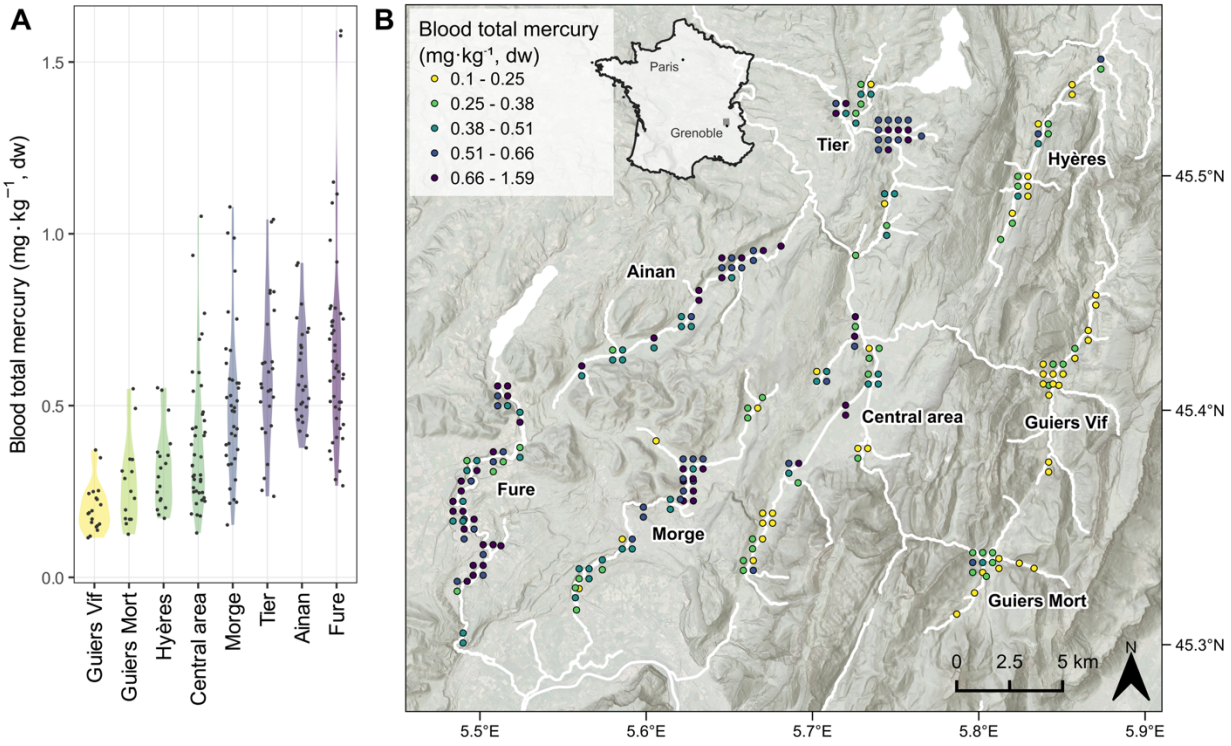


Fig. 1. Spatial variation in blood Hg in white-throated dippers across the study area (n = 229 samples from N = 199 birds, 2024–2025). *(A) Blood Hg (mg·kg^{-1} dry weight, dw) by river (Ainan, Central area, Fure, Guiers Mort, Guiers Vif, Hyères, Morge and Tier), with rivers ordered by increasing median blood Hg; violins show the distribution of concentrations and are shaded by the river median, and points show individual samples. (B) Capture locations in the Chartreuse Mountains, France, coloured by blood Hg class; points are slightly displaced to reduce overlap. The inset shows the location of the study area in France, with Paris and Grenoble for reference. The map was created in QGIS (sources: Ministère de la Culture France | Esri | Earthstar Geographics | TomTom | Garmin | NASA | NGA | USGS | METI/NASA | IGNF). Map lines do not necessarily depict accepted national boundaries.*

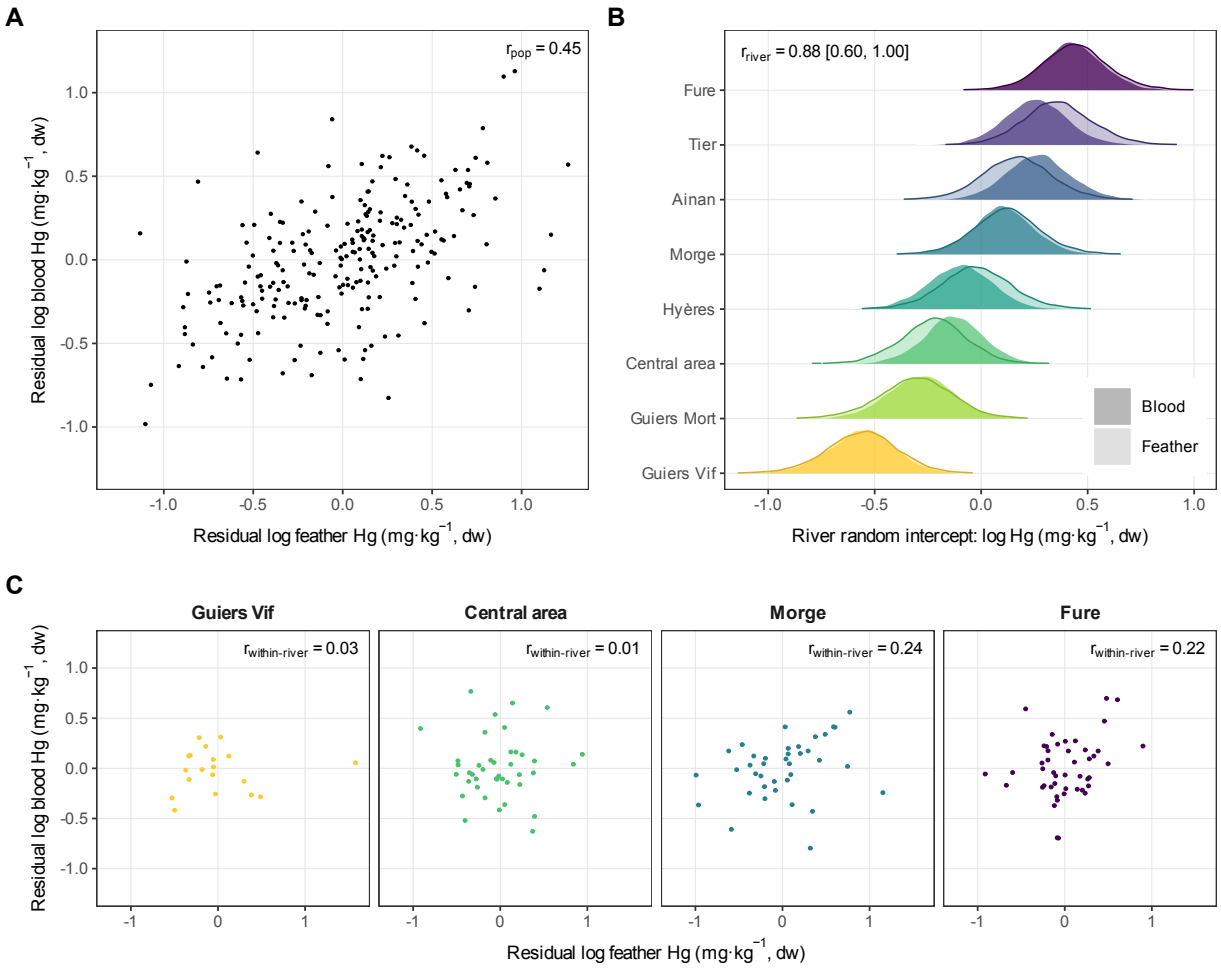


Fig. 2. Blood–feather Hg correlations at three spatial scales (aim ii; n = 229 samples from N = 199 birds). *All panels show log-transformed Hg (mg·kg^{-1} dw) from bivariate mixed-effects models; residuals are observed values minus the posterior mean of the expected value, that is, after the fixed and random effects of the respective model have been accounted for. (A) Population level: residual blood Hg against residual feather Hg for all samples (population model). (B) Among rivers: posterior distributions of the river-level random intercepts of the river-structured model for blood (darker shading) and feather Hg (lighter shading), expressed as deviations from the population mean; colours identify rivers, which are ordered by their mean intercept. (C) Within rivers: residual blood Hg against residual feather Hg of the river-structured model, after river-level structure has been removed, for four rivers (Guiers Vif, Central area, Morge, Fure) chosen to span low to high mean Hg; the value in each panel is that river's own within-river correlation (Table A.4), whereas the estimate pooled across all eight rivers is $r_{within-river}$ = 0.09. All correlations are reported in Table 2 and, for each river, in Table A.4.*

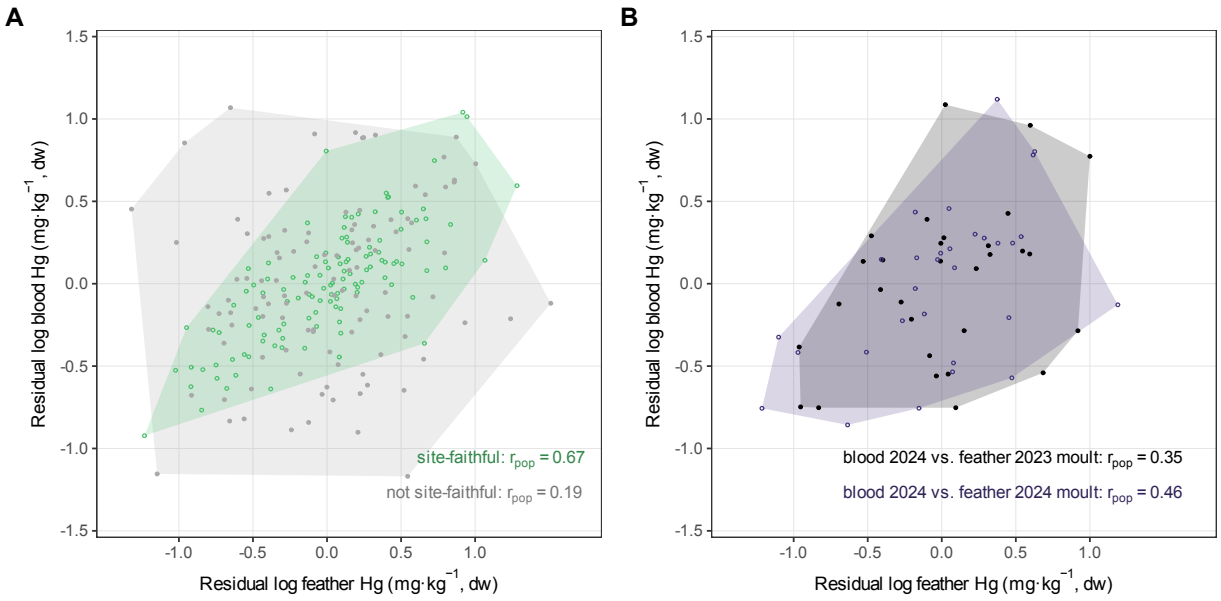


Fig. 3. Site fidelity and the timing of feather growth in relation to population-level blood–feather Hg correlations (aims iii and iv). *Axes show residual log-transformed Hg (mg·kg^{-1} dw) in paired blood and feather samples, after the fixed and random effects of the respective bivariate model have been accounted for. (A) Site fidelity: site-faithful birds, whose last known pre-moult location lay within 1 km of the capture location (green open circles, n = 118 samples; r_{pop} = 0.67), and birds that were not site-faithful (dark grey filled points, n = 111; r_{pop} = 0.19). (B) Timing of feather growth, for the 30 birds sampled in both years: blood Hg sampled in 2024 against Hg in the feather grown before blood sampling, that is, collected at the same capture and grown in the 2023 moult (black filled points; r_{pop} = 0.35), or in the feather grown after blood sampling, collected at the 2025 recapture and grown in the 2024 post-breeding moult (purple open circles; r_{pop} = 0.46). Shaded polygons are convex hulls around each group, both shown for visualisation only. Correlations are reported in Table 2.*

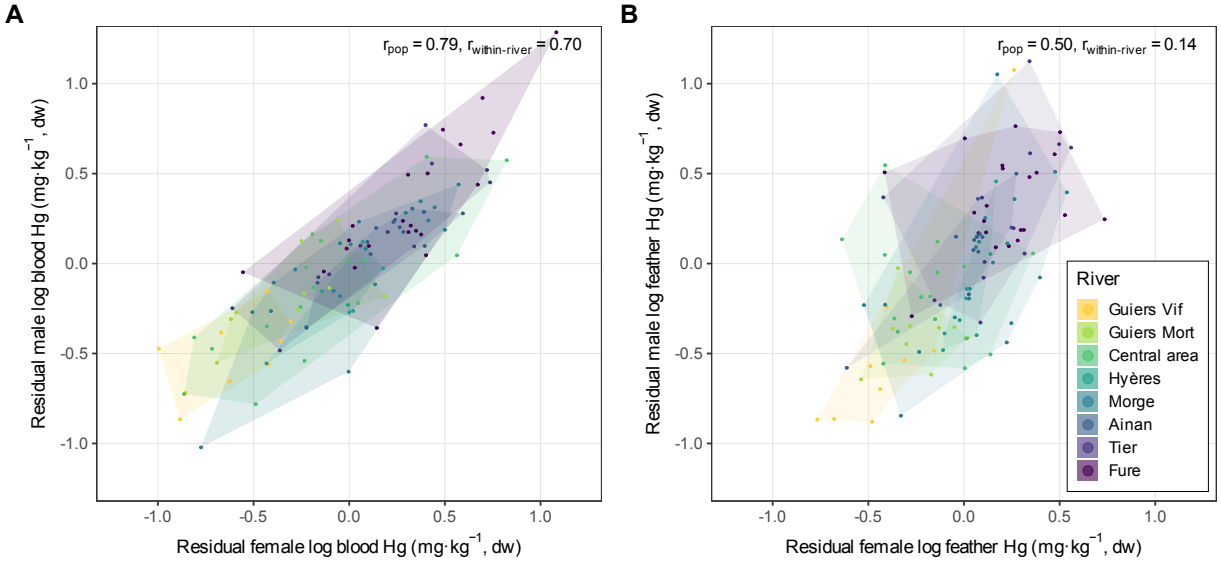


Fig. 4. Correlations in blood and feather Hg between the male and female member of a breeding pair (aim v; n = 110 pairs, N = 96 females and 96 males). *Axes show residual log-transformed Hg (mg·kg^{-1} dw) of the female (x-axis) and the male (y-axis) of each pair, after the fixed and random effects of the respective bivariate model (population model: female and male identity as random effects) have been accounted for, in (A) for blood and in (B) for feathers. Points and convex hulls are coloured by the river unit of the nest. All correlations are reported in Table 2.*

Appendix A. Supplementary data for

Spatial scale and site fidelity shape the correlation between blood and feather mercury in a riverine bird

Authors

Lara Hinninger[a,b,*], Molly Ohse[a,c], Blandine Doligez[d,‡], Pierre Bize[a,c,‡]

[a]*Swiss Ornithological Institute, Seerose 1, 6204 Sempach, Switzerland*

[b]*University of Zurich, Winterthurerstrasse 190, 8057 Zurich, Switzerland*

[c]*Department of Ecology and Evolution, University of Lausanne, Biophore, 1015 Lausanne, Switzerland*

[d]*Université Lyon 1, CNRS, LBBE, UMR 5558, Villeurbanne, France*

* Corresponding author. E-mail address: lara.hinninger@vogelwarte.ch

‡ Shared senior authorship

Contact + ORCIDs

L.H.: Lara Hinninger (lara.hinninger@vogelwarte.ch): 0009-0003-7490-4280

M.O.: Molly Ohse (molly.ohse@vogelwarte.ch): 0009-0006-2303-4723

P.B.: Pierre Bize (pierre.bize@vogelwarte.ch): 0000-0002-6759-4371

B.D.: Blandine Doligez (blandine.doligez@univ-lyon1.fr): 0000-0003-3015-5022

A.1 Sample collection, mercury analysis details and conversion of toxicity benchmarks

Blood was collected with a 27G 3/4″ single-use needle into a 300 µl Microvette® capillary tube (CB 300 LH, SARSTEDT, Nürnberg, Germany), kept on ice and processed within 17 h; plasma and red blood cells were separated by centrifugation and stored at −20 °C. Feathers were stored in sealed plastic bags in the dark at room temperature. For analysis, about 15 µl of thawed red blood cells were pipetted onto filter paper strips (Whatman™ Grade 4) and dried for 16 h in a desiccator at room temperature. Feathers were rinsed twice with deionised water, ultrasonicated in a 2% alkaline solution (RBS-50) for 5 min, rinsed again and dried overnight at 65 °C. Dry weights of both sample types were recorded before analysis. Samples were thermally decomposed at 950 °C; volatilised Hg was captured on a gold amalgamator and quantified by atomic absorption spectrometry at 253.7 nm.

Total mercury (Hg) concentrations were measured using the Direct Mercury Analyser (DMA-80 evo, Milestone Srl, Sorisole, Italy) at the cLab, Institute of Geography, University of Bern. The instrument is subject to regular maintenance, calibration, and performance checks according to institutional quality control procedures. Each analytical run comprised 30 samples and included analytical blanks at the beginning and end of the run. After every 10 biological samples, an empty sample boat, a certified reference material (CRM), and, for blood samples, a boat containing filter paper only were analysed to monitor potential contamination and analytical drift. For feather analyses conducted in 2024, we used lobster hepatopancreas (TORT-3), yielding a mean ± standard deviation (SD) recovery of 98.4 ± 5.5% (n = 42). In 2025, we used human hair (ERM-DB001) as CRM, with a recovery of 92.7 ± 3.9% (n = 20). All blood samples were analysed in 2025, and we used mussel tissue (NIST® 2976) as CRM, resulting in a recovery of 97.5 ± 4.0% (n = 30).

Analytical methods differed between the two sample matrices. Feather samples were analysed in nickel boats using the standard DMA method for solid materials (Table A.1). Blood samples were analysed in quartz boats, which are commonly used to improve analytical accuracy and precision. Method settings were adapted from protocols developed for the analysis of human and avian dried blood spots (González-Rubio et al., 2023; Perkins & Basu, 2018). The Hg contribution of the filter paper was subtracted from the total Hg measured in blood samples.

Table A.1. DMA-80 evo method parameters for feather and blood Hg analyses.

	Blood	**Feathers**
Sample type	Dried red blood cells on filter paper	Washed undertail covert feather
Sample weights (mean ± standard deviation)	Paper: 20.2 ± 1.4 mg; dried blood: 5.0 ± 0.9 mg	Feather: 3.2 ± 1.1 mg
Sample boat material	Quartz	Nickel
Maximum start temperature	200 °C	400 °C
Drying time	1 min	–
Temperature ramp	1 min	1 s
Decomposition temperature	950 °C	950 °C
Decomposition time	1.5 min	4 min
Purge time	1 min	1 min
Amalgamator time	12 s	12 s
Signal recording time	24 s	30 s
Total time	5 min 6 s	5 min 43 s

A.2 Overview table of all models

Table A.2 presents all Bayesian univariate (one response variable; i) and bivariate (two response variables; ii–v) mixed models used in this study. Models are ordered according to the study aims, which are indicated in the first column. Models met the convergence criteria (R-hat ≤ 1.01, bulk and tail effective sample sizes ≥ 400 of 12,000 draws). For aim i, ΔELPD (± standard error) relative to the model with the highest predictive accuracy was −0.9 ± 1.2 (interaction), −1.2 ± 0.7 (quadratic) and −4.4 ± 1.7 (full) for blood, where the linear model ranked first. For feathers, the quadratic model ranked first, followed by the linear (−0.3 ± 2.7), interaction (−1.5 ± 3.0) and full model (−2.6 ± 1.6). ELPD values for observations with Pareto k > 0.7 were obtained from exact refits (Section 2.4.1).

Table A.2. Overview of Bayesian models used to investigate log total mercury (Hg) concentrations in blood and feathers of white-throated dippers. *The table shows all main models used in the manuscript. For bivariate models, the random-effects column is divided into two columns: the left column shows the random effects in the population model used to estimate correlations at the population level, whereas the right column shows the random effects of the river-structured model used to estimate correlations among and within rivers. n = number of samples; N = number of individuals; f = female; m = male; ring = bird identity; × = interaction; Ixn = interaction model; Quad = quadratic model.*

Aim	Dataset	n (N)	Response	Fixed effects	Random effects	
i	all birds	229 (199)	blood Hg	Linear: age + date + sex + year	river | territory + ring	
			or	Quad: age^2 + $date^2$ + sex + year		
			feather Hg	Ixn: (age + date) × sex + year		
				Full: (age^2 + $date^2$) × sex + year		
					Population	*River-structured*
ii	all birds	229 (199)	feather Hg	sex + year	ring	river + ring
			blood Hg	date + year	ring	river + ring
iii	site-faithful	118 (103)	feather Hg	sex + year	ring	river + ring
			blood Hg	date + year	ring	river + ring
	not site-faithful	111 (108)	feather Hg	sex + year		river
			blood Hg	date + year		river
	older adults	128 (108)	feather Hg	sex + year	ring	river + ring
			blood Hg	date + year	ring	river + ring
	yearlings	101 (101)	feather Hg	sex + year		river
			blood Hg	date + year		river
iv	recaptured individuals	30 (30)	feather Hg (2023 moult)	sex		
			blood Hg 2024	date 2024		
		30 (30)	feather Hg (2024 moult)	sex		
			blood Hg 2024	date 2024		
					Population	*River-structured*
v	breeding pairs	110 (f, m = 96)	blood Hg female	date female + year	ring f	river + ring f
			blood Hg male	date male + year	ring m	river + ring m
		110 (f, m = 96)	feather Hg female	year	ring f	river + ring f
			feather Hg male	year	ring m	river + ring m

A.3 Univariate models without repeated individuals

We repeated the univariate models (aim i) with each bird included only once (n = N = 199). For each of the 30 birds sampled in both years, one of its two samples was selected at random; all other birds contributed their single sample. The bird-identity random effect could therefore be dropped, and territory variance could not be inflated by repeated sampling of the same bird. The variance structure closely matched that of the full dataset (Table 1). River and territory each accounted for a substantial share of the variance in blood Hg (ICC = 0.54 and 0.23, vs. 0.55 and 0.24 in the full dataset). Feather Hg, in contrast to blood, was structured mainly by river (ICC = 0.46 vs. 0.50), with little territory-level variance (ICC = 0.06 vs. 0.03; Table A.3).

Table A.3. Sources of variation in blood and feather Hg in a restricted dataset (aim i). *Parameter estimates (posterior mean, 95% highest density interval [HDI] and probability of direction [Pd]) from univariate Bayesian mixed-effects models of blood and feather total Hg, fitted to one randomly chosen sample per bird (n = N = 199; 105 territories, because four territories were represented only by samples that were not selected). The upper block reports fixed-effect posterior means with 95% HDI and Pd; the lower block reports random-effect standard deviations (SD) with 95% HDI, intra-class correlation coefficients (ICC) and Bayesian R^2. Values in bold indicate Pd ≥ 0.975.*

	log blood Hg (mg·kg^{-1} dw)			**log feather Hg (mg·kg^{-1} dw)**		
Fixed effects	Estimate	95% HDI	Pd	Estimate	95% HDI	Pd
Intercept	**−0.86**	**[−1.18, −0.53]**	**1.00**	**0.49**	**[0.15, 0.83]**	**1.00**
age	0.04	[−0.01, 0.09]	0.95	0.02	[−0.05, 0.08]	0.71
sex [male]	−0.07	[−0.15, 0.02]	0.94	−0.10	[−0.23, 0.02]	0.95
year [2025]	−0.10	[−0.20, 0.00]	0.97	−0.06	[−0.20, 0.08]	0.81
date	−0.17	[−0.23, −0.11]	1.00	0.02	[−0.06, 0.09]	0.67
Random effects	SD	95% HDI	ICC	SD	95% HDI	ICC
river (N = 8)	0.42	[0.18, 0.72]	0.54	0.42	[0.19, 0.73]	0.46
territory (N = 105)	0.27	[0.21, 0.33]	0.23	0.15	[0.00, 0.26]	0.06
Residual	0.27	[0.23, 0.31]		0.44	[0.38, 0.49]	
$R^2_{conditional}$ / $R^2_{marginal}$	0.76 / 0.14			0.40 / 0.03		

A.4 Mercury concentrations and blood–feather correlations by river

The within-river correlation in Table 2 is a single estimate pooled across all eight rivers ($r_{within\text{-}river}$ = 0.09). To examine how it varied among rivers, we took the observation-level residuals of the same model (river-structured model, Section 2.4.2) and, in every posterior draw, computed the blood–feather correlation separately within each river. For these computations no models were refitted. River-specific estimates were imprecise and ranged from −0.17 (Ainan) to 0.24 (Morge; Table A.4). Only Morge reached our evidence threshold for a positive within-river correlation (Pd = 0.98), and Fure provided weak evidence (Pd = 0.97); the remaining six rivers showed no clear evidence of a correlation in either direction. All river-specific HDIs included the pooled estimate, so we found no clear evidence that the correlation differed among rivers; with only eight rivers, these comparisons are descriptive.

Table A.4. River-specific mercury concentrations and within-river blood–feather Hg correlations (aim ii). *For each river, the table gives mean blood and feather Hg (raw data, mg·kg^{-1} dw) and the within-river correlation (r) between blood and feather Hg. Correlations are posterior means [95% highest density interval, HDI] with probability of direction (Pd), obtained by splitting the observation-level residuals of the river-structured mode (aim iii)l, rather than by refitting the model for each river. SD blood and SD feather are the within-river residual standard deviations of log-transformed Hg (posterior means). Rivers are ordered by increasing r. Values in bold indicate Pd ≥ 0.975. n = number of samples; N = number of individuals.*

		Raw data (mg·kg^{-1} dw)		**Model data**			
River	**n (N)**	Blood Hg	Feather Hg	$r_{within\text{-}river}$ [95% HDI]	Pd	SD blood	SD feather
Ainan	26 (21)	0.60	1.75	−0.17 [−0.50, 0.21]	0.82	0.23	0.33
Guiers Mort	15 (15)	0.27	1.16	−0.06 [−0.43, 0.32]	0.64	0.31	0.32
Hyères	18 (18)	0.32	1.58	−0.04 [−0.40, 0.35]	0.58	0.25	0.34
Central area	41 (35)	0.40	1.26	0.01 [−0.20, 0.22]	0.52	0.35	0.40
Guiers Vif	19 (16)	0.20	1.04	0.03 [−0.28, 0.30]	0.59	0.26	0.50
Tier	26 (20)	0.59	2.54	0.10 [−0.15, 0.34]	0.81	0.32	0.45
Fure	46 (39)	0.67	2.48	0.22 [0.01, 0.40]	0.97	0.34	0.37
Morge	38 (35)	0.51	1.94	**0.24 [0.02, 0.43]**	**0.98**	0.34	0.49

A.5 Sensitivity to the site-fidelity threshold

Site-faithful birds were defined as birds captured within 1 km along the river of their moult location (Section 2.4.2). To test whether the contrast between site-faithful and not site-faithful birds depended on this threshold, we repeated the classification with thresholds of 0.5, 2 and 5 km and refitted the bivariate models (aim iii) to each group (Table A.5). Birds were reclassified by their distance along the river where this distance was known; birds without a proxy for the moult location, or whose locations were not connected along the mapped rivers, remained not site-faithful, as in the main analysis. Correlations in site-faithful birds were stable across thresholds (r_{pop} = 0.63 to 0.68), and the population-level correlation was higher in site-faithful than in not site-faithful birds at every threshold (Δ = 0.47 to 0.58, Pd = 1.00). Within rivers, the difference had the same direction (Δ = 0.28 to 0.43, Pd = 0.97 to 0.99), but its interval included zero at 0.5 and 2 km, and among rivers the difference remained uncertain (Pd = 0.85 to 0.96). With increasing threshold, the not site-faithful group became smaller (n = 128, 111, 92 and 64 for 0.5, 1, 2 and 5 km) and consisted increasingly of birds without a proxy for the moult location (44 of 64 samples at 5 km), so that its estimates at high thresholds are less informative about birds that moulted far away.

Table A.5. Sensitivity of the blood–feather correlations of site-faithful and not site-faithful birds to the distance threshold defining site fidelity (aim iii). *Correlations (r; posterior mean [95% HDI]) and probability of direction (Pd) of each correlation and of the difference Δ (site-faithful minus not site-faithful) from bivariate Bayesian mixed-effects models at three spatial scales, fitted separately to each group (population level, r_{pop}; among rivers, r_{river}; within rivers, $r_{within\text{-}river}$). Birds were classed by their distance along the river between capture and moult location where it was known; for birds without a known distance, the class of the main analysis was kept. The 1 km rows are the main analysis (Table 2). Values in bold indicate Pd ≥ 0.975. n = number of samples; N = number of individuals. Bird identity was included as a random effect only in groups with at least ten birds sampled in both years, i.e. in all site-faithful groups (13, 15, 19 and 24 birds at 0.5, 1, 2 and 5 km) but in none of the not site-faithful groups (5, 3, 1 and 0 birds).*

Correlations (r)		Population level (r_{pop})		Among rivers (r_{river})		Within-river ($r_{within\text{-}river}$)	
Threshold	n (N)	mean [95% HDI]	Pd	mean [95% HDI]	Pd	mean [95% HDI]	Pd
0.5 km							
site-faithful	101 (88)	**0.68 [0.54, 0.82]**	**1.00**	**0.90 [0.62, 1.00]**	**1.00**	**0.33 [0.05, 0.58]**	**0.98**
not site-faithful	128 (123)	**0.22 [0.05, 0.38]**	**1.00**	0.63 [0.05, 1.00]	0.96	0.00 [−0.18, 0.18]	0.52
difference Δ		**0.47 [0.24, 0.68]**	**1.00**	0.27 [−0.27, 1.02]	0.85	0.32 [−0.01, 0.64]	0.97
1 km							
site-faithful	118 (103)	**0.67 [0.54, 0.81]**	**1.00**	**0.91 [0.68, 1.00]**	**1.00**	**0.35 [0.12, 0.56]**	**1.00**
not site-faithful	111 (108)	**0.19 [0.01, 0.37]**	**0.98**	0.58 [−0.04, 1.00]	0.94	−0.01 [−0.20, 0.18]	0.55
difference Δ		**0.48 [0.25, 0.71]**	**1.00**	0.33 [−0.19, 1.09]	0.90	**0.36 [0.06, 0.65]**	**0.99**
2 km							
site-faithful	137 (118)	**0.63 [0.51, 0.76]**	**1.00**	**0.91 [0.65, 1.00]**	**1.00**	**0.29 [0.10, 0.50]**	**1.00**
not site-faithful	92 (91)	0.15 [−0.05, 0.35]	0.93	0.36 [−0.36, 0.95]	0.82	0.02 [−0.19, 0.24]	0.56
difference Δ		**0.48 [0.24, 0.72]**	**1.00**	0.54 [−0.11, 1.39]	0.95	0.28 [−0.01, 0.56]	0.97
5 km							
site-faithful	165 (141)	**0.63 [0.50, 0.75]**	**1.00**	**0.93 [0.72, 1.00]**	**1.00**	**0.30 [0.12, 0.49]**	**1.00**
not site-faithful	64 (64)	0.05 [−0.20, 0.29]	0.65	0.35 [−0.39, 1.00]	0.80	−0.13 [−0.39, 0.13]	0.82
difference Δ		**0.58 [0.30, 0.85]**	1.00	0.57 [−0.07, 1.45]	0.96	**0.43 [0.11, 0.75]**	0.99

A.6 Blood–feather correlations in age class groups

Site fidelity and age class were closely linked in our population: 110 of the 118 samples from site-faithful birds came from older adults, and 93 of the 101 yearling samples came from birds that were not site-faithful. To test whether age class can serve as a field proxy for site fidelity, we repeated the bivariate models (aim iii) with age class instead of site fidelity. Yearlings were in their first breeding season and were therefore sampled only once (n = N = 101), so bird identity was omitted from their models; all other settings were as in Section 2.4.2. Correlations were stronger in older adults than in yearlings at the population level (r_{pop} = 0.60 vs. 0.22; Δ = 0.37 [0.13, 0.60]) and within rivers ($r_{within\text{-}river}$ = 0.29 vs. −0.01; Δ = 0.30 [0.01, 0.59]), but not clearly among rivers (Δ = 0.30 [−0.27, 1.08]; Table A.6). These differences were slightly smaller than those between site-faithful and not site-faithful birds (Table 2). Because the two classifications differed for only 26 samples (18 older adults that were not site-faithful and 8 site-faithful yearlings), this analysis cannot show whether age or site fidelity underlies the pattern. It does show, however, that age class reproduces the contrast and can therefore serve as a practical field proxy where moult locations are unknown.

Table A.6. Blood–feather Hg correlations in age class groups (aim iii). *Correlations (r; posterior mean [95% HDI]) and probability of direction (Pd) from bivariate Bayesian mixed-effects models at three spatial scales, fitted separately for older adults and yearlings. Δ is older adults minus yearlings. Values in bold indicate Pd ≥ 0.975. n = number of samples; N = number of individuals.*

Correlations (r)		Population level (r_{pop})		Among rivers (r_{river})		Within-river ($r_{within\text{-}river}$)	
Aim	n (N)	mean [95% HDI]	Pd	mean [95% HDI]	Pd	mean [95% HDI]	Pd
Blood–feather Hg correlations							
(iii) *age groups*							
older adults	128 (108)	**0.60 [0.46, 0.74]**	**1.00**	**0.90 [0.63, 1.00]**	**1.00**	**0.29 [0.08, 0.49]**	**1.00**
yearlings	101 (101)	**0.22 [0.02, 0.40]**	**0.99**	0.60 [0.01, 1.00]	0.95	−0.01 [−0.22, 0.19]	0.53
difference Δ		**0.37 [0.13, 0.60]**	**1.00**	0.30 [−0.27, 1.08]	0.87	**0.30 [0.01, 0.59]**	**0.98**

A.7 Sensitivity of the feather correlation between breeding partners to the distance between their moult locations

Feathers record where each bird moulted, and the partners of many pairs had moulted apart (Section 4.4). If this explains why partners resemble each other less in feather than in blood Hg, the feather correlation should rise in pairs that had moulted close together. To test this, we refitted the feather models (aim v) to subsets of pairs whose moult locations lay within 1, 2 or 5 km of each other along the river, and to pairs whose moult locations lay in the same river (Table A.7). Pairs for which the moult location of one partner was unknown, or the two locations were not connected along the mapped rivers, were not included in any subset. Individual random effects were omitted because fewer than ten females or fewer than ten males per subset were sampled in both years. All other settings were as in Section 2.4.3. The correlations did not increase in the subsets: the population-level correlation was not higher (r_{pop} = 0.34 to 0.42, against 0.50 for all pairs), and the within-river correlation remained close to zero even for pairs that had moulted within 1 km of each other ($r_{within\text{-}river}$ = −0.07 [−0.42, 0.29]). The subsets were small (39 to 67 pairs), so their intervals are wide, and the among-river correlations, which rest on eight rivers, were imprecise.

Table A.7. Feather Hg correlation between the two members of a breeding pair in subsets of pairs defined by the distance between the partners' moult locations (aim v). *Correlations (r; posterior mean [95% HDI]), probability of direction (Pd) from bivariate Bayesian mixed-effects models at three spatial scales (population level, r_{pop}; among rivers, r_{river}; within rivers, $r_{within\text{-}river}$). Rivers refer to the pair's nest location. Subsets are nested (0.5 km within 1 km within 2 km within 5 km) and were fitted without individual random effects. The first row (all pairs) is the analysis from the main models (Table 2), which include individual random effects. n: number of samples, N: number of individuals (f = females, m = males). Values in bold indicate Pd ≥ 0.975.*

Correlations (r)		Population level (r_{pop})		Among rivers (r_{river})		Within-river ($r_{within\text{-}river}$)	
Subset	n (N)	mean [95% HDI]	Pd	mean [95% HDI]	Pd	mean [95% HDI]	Pd
All pairs	110 (f = m = 96)	**0.50 [0.25, 0.76]**	**1.00**	**0.77 [0.29, 1.00]**	**0.99**	0.14 [−0.12, 0.40]	0.85
1 km	39 (f = 35, m = 34)	**0.35 [0.06, 0.62]**	**0.99**	0.73 [0.16, 1.00]	0.97	−0.02 [−0.36, 0.32]	0.55
2 km	51 (f = m = 45)	**0.37 [0.13, 0.61]**	**1.00**	**0.78 [0.26, 1.00]**	**0.98**	0.05 [−0.24, 0.35]	0.64
5 km	62 (f = 55, m = 54)	**0.41 [0.19, 0.61]**	**1.00**	**0.79 [0.30, 1.00]**	**0.99**	0.09 [−0.18, 0.35]	0.75
Same river	67 (f = 58, m = 57)	**0.42 [0.22, 0.62]**	**1.00**	**0.80 [0.34, 1.00]**	**0.99**	0.10 [−0.15, 0.35]	0.79

References

González-Rubio, J. M., Domínguez-Morueco, N., Pedraza-Díaz, S., Cañas Portilla, A., Lucena, M. Á., Rodriguez, A., Castaño, A., & Esteban-López, M. (2023). A simple method for direct mercury analysis in dried blood spots (DBS) samples for human biomonitoring studies. *Environment International*, *177*, 107958. https://doi.org/10.1016/j.envint.2023.107958

Perkins, M., & Basu, N. (2018). Dried blood spots for estimating mercury exposure in birds. *Environmental Pollution*, *236*, 236–246. https://doi.org/10.1016/j.envpol.2018.01.036